AAPS PharmSciTech, Vol. 15, No. 4, August 2014 (© 2014)
DOI: 10.1208/s12249-014-0105-z

Research Article

An Explanation for the Difference in the Percutaneous Penetration Behavior of Tamsulosin Induced by Two Different *O*-Acylmenthol Derivatives

Lei Shang,[1] Dongmei Cun,[1] Honglei Xi,[1] and Liang Fang[1,2]

Received 11 November 2013; accepted 23 February 2014; published online 22 March 2014

Abstract. Using tamsulosin (TAL) as a model drug, the aim of this study was to investigate and compare the percutaneous permeation behavior of two menthol derivatives, 2-isopropyl-5-methylcyclohexyl heptanoate (M-HEP) and 2-isopropyl-5-methylcyclohexyl decanoate (M-DEC). *In vitro* transdermal permeation study was carried out using porcine skin. The residual amount of enhancers in the skin after permeation experiment was determined by gas chromatographic (GC) method. The penetration depths of fluorescein were visualized by two-photon confocal laser scanning microscopy (2P-LSM) after the skin being treated with different enhancers. Furthermore, changes in the stretching frequency of functional group of ceramide were investigated by using attenuated total reflectance Fourier transform infrared (ATR-FTIR) technique. After M-HEP addition, the cumulative amount of TAL permeated in 8 h (Q_8) reached 20.57±0.54 μg/cm^2 and the depth of fluorescein was 40 μm; the CH_2 of ceramide symmetric stretching frequency was 4 cm^{-1} blue shifted. However, M-DEC has an opposite effect on TAL permeation compared with that of M-HEP. TAL is a crucial factor affecting permeation procedure, and microenvironment of lipid region determines promotion capability of the enhancers.

KEY WORDS: enhancer; mechanism; menthol derivative; retardant; transdermal.

INTRODUCTION

The discovery of new penetration enhancers with high efficiency and low toxicity is of great importance to the development of transdermal drug delivery system. Menthol, a frequently used percutaneous enhancer, is superior to many other chemical enhancers due to its outstanding safety. Menthol is naturally sourced and generally recognized as safe (GRAS) by FDA. Unfortunately, the volatility of menthol is a disadvantage for transdermal administration. In our previous studies, a series of menthol derivatives were synthesized and their ability to enhance the percutaneous permeation of 5-fluorouracil, isosorbide dinitrate, lidocaine, ketoprofen, and indomethacin were evaluated (1–3). Some of the menthol derivatives have exhibited favorable enhancing activities. However, in the current study, when two menthol derivatives, 2-isopropyl-5-methylcyclohexyl heptanoate (M-HEP) and 2-isopropyl-5-methylcyclohexyl decanoate (M-DEC) (Fig. 1), were used as enhancers for transdermal delivery of tamsulosin (TAL) (Fig. 2), the results showed that M-HEP could promote the permeation of TAL through the porcine skin, while M-DEC exhibited retardation effect. This phenomenon was unexpected since the structure of M-HEP and M-DEC is almost the same and the only difference between them is that the hydrocarbon chain of M-DEC contains three more methylene groups than that of M-HEP. The opposite behavior of these two derivatives in penetration enhancement might be attributed to their difference in molecular size. It is highly desirable to better understand their individual permeation mechanisms to provide us with the theoretical basis for future evaluation of other menthol derivatives.

As reported in the literatures, the penetration-enhancing behavior of oleic acid and *O*-ethylmenthol has been successfully investigated using two-photon confocal laser scanning microscopy (2P-LSM) (4–6). Sulforhodamine B and rhodamine B hexyl ester have been used as the probe to study oleic acid-induced change in skin structure and permeation behavior. In addition, the attenuated total reflectance Fourier transform infrared (ATR-FTIR) mode has provided insights into the vibration frequencies of ceramide (CER) in the intact stratum corneum (SC) (7–9). Unfortunately, most of these studies concentrated on the interaction between the enhancer and skin but ignored the potential effect on penetrant characteristics, which is a crucial factor in the penetration process. It is known that the interaction between penetrant characteristics and ceramide or enhancer can affect the efficiency of promoter. Therefore, it is absolutely essential to take the penetrant characteristics into account during enhancer mechanism investigation. Moreover, few studies have explained the reason why some compounds could reversely inhibit the penetration of drugs through the skin.

Therefore, the purpose of this study is to elucidate the reason for the opposite behavior of M-DEC and M-HEP

[1] Department of Pharmaceutical Sciences, Shenyang Pharmaceutical University, 103 Wenhua Road, Shenyang, 110016Liaoning, China.
[2] To whom correspondence should be addressed. (e-mail: fangliang2003@yahoo.com

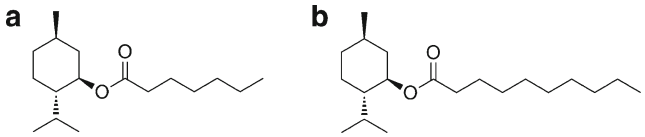

Fig. 1. The image of chemical structures of M-HEP (**a**) and M-DEC (**b**)

when both of them are used as penetration enhancers of TAL. First of all, *in vitro* penetration experiment and gas chromatograph (GC) analysis provided direct information about their enhancing efficiency and retention amount of M-DEC or M-HEP in the skin. Then, 2P-LSM was applied to visualize the penetration of fluorescent penetrant in the skin in the presence of M-HEP or M-DEC. The conformation variation of CER, the main composition of skin lipid, was shown in ATR-FTIR spectra after application of M-HEP and M-DEC, which was expected to provide additional information to elucidate the penetration mechanism of M-HEP and M-DEC.

MATERIALS AND METHODS

Materials

TAL hydrochloride was purchased from Wuhan He Zhong Pharmaceutical Co., Ltd. (Hubei, China); TAL was prepared based on pH adjustment method and identified by DSC method; isopropyl myristate (IPM) and L-menthol were supplied by China National Medicine Co., Ltd. (Shanghai, China). Methanol of HPLC grade was purchased from Yuwang Pharmaceutical Co., Ltd. (Shandong, China). M-HEP and M-DEC (the purities of M-HEP and M-DEC are up to 98%) were synthesized and purified according to our previous work (Zhao *et al.*, 2008a; Zhao *et al.*, 2008b). The fluorescein was purchased from Acros Organics (NJ, USA). All other chemicals and solvents were of analytical grade.

Skin Sample Preparation

The procedure of skin preparation was conducted in accordance with the Ethical Guidelines for Investigations in Laboratory Animals and was approved by the Ethics Review Committee for Animal Experimentation of Shenyang Pharmaceutical University. The miniature pigs were obtained from Chongqing Zongshen Biological Technology Research and Development of Medical Co., Ltd. (Chongqing, China). After sacrificed, the abdominal skin was excised and the adhering fat was removed. The thickness of the full skin was about 700 μm. And then, the skin was cleaned with cold running water to remove the dried blood and dirt. The integrity of the skin was checked by microscopy, and thereafter, the skin was ready for use.

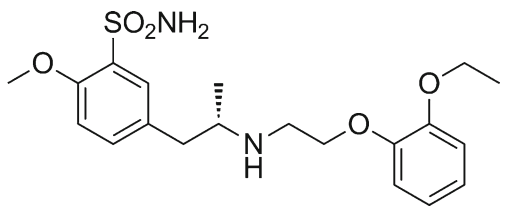

Fig. 2. The image of chemical structure of tamsulosin (TAL)

In Vitro Permeation Study

Skin permeation experiments were performed according to the method described by Fang *et al.* (10). In brief, the porcine skin was mounted between two chambers of a side-by-side glass diffusion cell with an effective diffusion area of 0.95 cm^2 and the temperature was maintained at 32°C by connecting the device to a water bath via a water jacket to mimic the physiological skin condition. The donor compartment was filled with 3.0 ml of TAL suspensions in IPM. The TAL suspensions with or without 20% M-HEP or 20% M-DEC (20% concentration of total donor volume, *v*/*v*) existed in the donor compartment. Excessive amount of TAL was added into the donor phase to maintain the saturation condition of the drug in the donor phase, and the receptor compartment was filled with 3 ml of phosphate buffer solution (PBS, pH at 7.4) as receptor medium. Both donor and receptor phases were continuously stirred at about 600 rpm. At 1, 2, 3, 4, 5, 6, 7, and 8 h, 2.0 ml of receptor solution was withdrawn for analysis and replaced with the same volume of fresh medium to maintain sink conditions.

The cumulative amount of TAL passing across porcine skin was calculated based on the measured drug concentration in the receiver medium. The accumulative amount of TAL permeating through the skin was calculated according to the following equation:

$$Q = \left(C_i \times V + \sum_{i=1}^{n-1} C_{i-1} \times V_i \right) / A \quad i = 1, 2, 3 \tag{1}$$

where Q is the cumulative amount of the drug transported across the skin, C_i is the drug concentration in the receiver compartment, and V is the volume of the receptor compartment. V_i is the volume of the sample for analysis. The cumulative penetration amount of TAL was plotted as a function of time.

After the completion of permeation experiment, the retention amounts of TAL and enhancer (M-DEC or M-HEP) in the skin were also determined. Accurately weighed skin was cut into small pieces, and the chemicals inside the skin were extracted by adding 1 ml of methanol and then treated in an ultrasound bath for 20 min. The content of TAL and enhancer in the sample was determined by HPLC and GC, respectively.

Determination of Drug and Fluorescein Solubility and Calculation of Solubility Parameter

To determine the saturated solubility of TAL or fluorescein in donor solution, excessive amount of drug or fluorescein was added to the vehicle. After being vortexed for 2 min and then sonicated for 10 min, the sample was shaken at 32± 0.5°C. After 48 h, the sample was filtered through a 0.45-μm membrane filter and the concentration of TAL or fluorescein in the filtrate was determined by HPLC. The experiments were repeated for four times.

The Hansen solubility parameters of TAL, M-HEP, and M-DEC were calculated based on their average molecular weight according to the approaches of Hoftyzer/Van Krevelen (Krevelen and Krevelen, 1990). The unit of solubility parameters is $(J\ cm^{-3})^{1/2}$ (11).

HPLC Determination

A validated HPLC method was developed to determine the concentration of TAL. The mobile phase is water:methanol (50:50, *v*/*v*), with pH adjusted to 6.5 (ethyl acetate triethylamine buffer), flow rate is 1 ml/min, and oven temperature is 40°C. Drug concentration in the withdrawn samples was calculated according to a calibration curve.

GC Determination

A validated GC method was developed to determine the amount of M-HEP and M-DEC retained in the skin. The gas chromatography (GC-17A) was equipped with a flame ionization detector (Shimadzu Corporation, Kyoto, Japan). Nitrogen was used as a carrier gas at a flow rate of 3.5 ml/min. A split injection (split ratio=20) was used where injector temperature, FID temperature, and column oven temperature were 250, 280, and 280°C, respectively. Concentrations of M-HEP and M-DEC in the samples were calculated by using the absolute calibration method.

Visualizing the Penetration of Fluorescein in Skin by 2P-LSM

In this experiment, a full-thickness porcine skin was mounted between two chambers of a Franz cell by clamping. A suspension of fluorescein in IPM with or without 20% M-HEP or 20% M-DEC and PBS buffer were used as the donor solution and receiver solution, respectively.

The experiment allowed the fluorescein to penetrate through the skin under 32°C. One hour later, the porcine skin was taken off from the device, washed three times with physiological saline, and then gently wiped with filter paper; treated area of the skin was cut out. Subsequently, the skin was positioned on a glass slide with the SC side upward. The fluorescent images of skin section at different z axis positions were obtained with a Zeiss LSM 710 microscope (Heidelberg, Germany) using a W Plan-Apochromat ×20/1.0 objective and a Coherent Chameleon Ultra laser tuned to 780 nm. TPM imaging was conducted based on a preliminary experiment and previously published methods (12). Each image was repeated for four times.

ATR-FTIR Study

Full porcine skin sample with thickness of about 700 μm was mounted between two Franz cells. Using IPM with or without 20% M-HEP or 20% M-DEC as donor solutions and PBS buffer as receiver medium, the skin was collected after a 1-h permeation process at 32±0.5°C. The skin surface was wiped cleanly with cotton swab; thereafter, the skin was placed on the surface of crystal with SC side down. The ATR-FTIR spectra of the samples were recorded in the frequency range of 4,000–500 cm^{-1} using an IR spectrometer (NEXUS+70, Thermo Electron Corporation, Waltham, MA, USA). The spectrum of the control sample was also recorded.

Data Statistics

All experiments were replicated at least four times. All data were calculated and presented as mean±SE. Statistical analysis was carried out using analysis of variance (ANOVA). The level of significance was determined as $P<0.05$.

RESULTS

In Vitro Porcine Skin Permeation of TAL with M-HEP or M-DEC

The effect of M-HEP or M-DEC on the permeation of TAL through porcine abdominal skin was examined. When there was no enhancer in the donor solution, the cumulative amount of TAL permeated per unit skin surface area in 8 h ($Q_{8\ h}$) reached 10.20±0.79 μg/cm^2 with 3.92 h of lag time. The addition of 20% M-HEP in the donor solution significantly increased $Q_{8\ h}$ of TAL to 20.57±0.54 μg/cm^2 ($P<0.05$), and the lag time was eliminated completely. Unexpectedly, the $Q_{8\ h}$ of TAL was nearly down to zero when 20% M-DEC was added in the donor phase. The obtained results indicated that the presence of M-DEC retarded the permeation of TAL significantly.

The Solubility of TAL and Fluorescein

The solubility of TAL and fluorescein in different vehicles was measured, and the results are shown in Table I. According to the method proposed by Hoftyzer/VanKrevelen (13), the calculated solubility parameters, δ, of M-HEP, M-DEC, and TAL are 17.28, 17.15, and 21.35$(J\ cm^{-3})^{1/2}$, respectively.

The Retention Amount of M-HEP or M-DEC in the Skin

The retention amount of potential enhancers in the skin after 8 h of permeation was measured by the GC method. It was shown that the retention amount of M-HEP is about 2.5-fold higher than that of M-DEC (Table I). Obviously, the higher the remaining amount of potential enhancers in the skin, the higher the amount of TAL permeated through the skin.

Visualization of the Penetration of Fluorescein in the SC by 2P-LSM

As a substitute for TAL, the penetration of fluorescein inside the skin could be visualized by 2P-LSM. As shown in Fig. 3, the black regions surrounded by the intercellular green fluorescence depicted the SC cell shape. As observed, the green fluorescent light of fluorescein was detectable at the depth of 40 μm away from the skin surface when 20% of M-HEP was added into the donor phase. However, fluorescent signal disappeared at the position deeper than 8 μm when 20% of M-DEC was incorporated into the donor phase. For the control group without enhancer, the deepest position that the fluorescein could reach in SC was 12 μm. It was obvious that M-HEP could enhance while M-DEC would retard the penetration of fluorescein.

Table I. Permeation Parameters of TAL and Fluorescein Through Porcine Skin

Vehicle (*w/w*) (10% ethanol/IPM)	TAL solubility (μg/ml)	Fluorescein solubility (μg/ml)	TAL retention amount (μg/g)	Modifier retention amount (μg/g)
Vehicle	137.64±10.10	96.31±9.49	90.98±8.73	–
20% M-HEP vehicle	148.83±9.12	157.34±11.12	150.71±12.87	15.87±2.31
20% M-DEC vehicle	100.23±8.76	90.87±10.97	29.67±4.43#*	6.14±1.03*

# *P<0.05, value is significantly different between 20% M-DEC vehicle control group*
**P<0.05, value is significantly different between 20% M-HEP vehicle control group*

ATR-FTIR

ATR-FTIR studies were performed to gain further information about the effect of M-HEP or M-DEC on the biophysical properties of the SC lipid region. ATR-FTIR spectra of porcine SC that has been pretreated with different donor phases containing TAL suspension with or without M-HEP or M-DEC are presented in Fig. 4. As can be seen, SC pretreated with M-HEP produced a higher shift in asymmetric and symmetric C–H vibration peak positions (ν_s 2,852 cm^{-1} and ν_{as} 2,922 cm^{-1}, respectively) in comparison with that of control (ν_s 2,848 cm^{-1} and ν_{as} 2,921 cm^{-1}, respectively). And the amide bond vibrations II of M-HEP is red shifted compared with that of control (1,547 *vs.* 1,549 cm^{-1}). However, there was no detectable change in C–H vibration peak position of SC with the 20% M-DEC group compared with control.

DISCUSSION

The mechanism of M-HEP or M-DEC on the permeability of TAL through porcine skin is very complicated, and generally, it is highly related to the interaction among the enhancer, the penetrant, and skin. Since the solubility parameter of TAL ($21.35(J\ cm^{-3})^{1/2}$) is similar to that of the skin ($20.5(J\ cm^{-3})^{1/2}$) (14), it was assumed that TAL could dissolve freely in the SC lipid. According to the calculated solubility parameter, the δ of M-HEP is $0.13(J\ cm^{-3})^{1/2}$ higher than that of M-DEC, implying that M-DEC might be dissolved in the lipid region easier than M-HEP. In addition, GC analysis indicated that 2.5 times more M-HEP was retained in the skin compared with that of M-DEC. Considering that the percentage of lipid composition in SC is very low, the existence of large amount of M-HEP could change the microenvironment by changing the solubility parameter of the lipid region. Consequently, the interaction between TAL and CER (the main ingredient of SC lipid) was weakened and TAL could be released from the lipid of SC layer and continuously passed through skin and went into the receiver medium accumulatively. In contrast, M-DEC was not able to change the microenvironment of the lipid region due to its low retention amount in the skin.

So far, there is no clear interpretation about the action site of menthol derivatives. 2P-LSM was employed to investigate the action site of these enhancers after application of M-HEP and M-DEC. The action path of M-HEP and M-DEC in the porcine skin samples is illustrated directly by 2P-LSM. In previous researches, 2P-LSM has been employed to evaluate the skin permeation of drugs (15,16). Since the penetrant is regarded as a crucial factor of the penetration process, it is necessary to take the effect of the penetrant into account. To the best of our knowledge, some similar experiments have ignored to choose appropriate fluorescent reagents, which cannot reflect the penetration process (4,5,7,17). Considering molecular weight and log *P* being crucial factors of transdermal procedure, this research selects a suitable fluorescence agent which possesses similar characteristics with TAL. The molecular weight of TAL free base is 408.48 and log *P* 2.2. The properties of fluorescein (molecular weight 332.31 and log *P* 2.68) are similar with those of TAL. To some extent, fluorescein can reflect the transdermal behavior of TAL. Thus, the results could simulate the transdermal process of TAL. In this research, clear 2P-LSM topographies of the skin were used to clarify the acting sites of M-HEP and M-DEC. The black regions surrounded by the intercellular green fluorescence depicted the SC cell shapes. And the images reflected that the major acting site of enhancers is continuous intercellular lipid domain. From the images, a weak fluorescence was localized within corneocytes of SC treated by M-HEP, while there was no fluorescence localized within corneocytes of SC after M-DEC treatment. Moreover, the penetration depth of the fluorescence into the skin is less than that of the control after M-DEC treatment, indicating that M-DEC retarded fluorescence penetration or M-DEC interacted with fluorescence. The 2P-LSM images showed that the major action domain was intercellular lipid region, and there were obviously different influences between M-HEP and M-DEC.

Previous studies have suggested that a chemical enhancer targeting the SC lipid region to enhance skin permeation requires the enhancer to orient itself within that microenvironment to perturb and alter the SC lipid lamellae structure (18,19). In order to reflect the actual effect of M-HEP and M-DEC in the permeation procedure, TAL was applied in the pretreatment process for ATR-FTIR experiment. After the pretreatment procedure, ATR-FTIR could reflect the vibration frequency of CER in SC under the circumstance of TAL and enhancers, which provided the explanation for the enhancing mechanism considering the effect of the penetrant.

It was reported that the hydrogen bonding made the lipid bilayer stable and enhanced the barrier characteristic of SC (20,21). When the CER net was distorted by the enhancers possessing a functional group, the hydrogen bonding of the trans-conformations of CER could be affected. Figure 2 shows the CH_2 stretching frequency after the application of M-HEP or M-DEC. Compared with the control group, the spectrum of the 20% M-HEP group presented an obvious blue shift. The symmetric stretch was a sensitive signal to the alkyl chain conformation. And the CH_2 symmetric stretching frequency was 4 cm^{-1} blue shifted. The magnitude of the shift in C–H stretching vibration was directly related to the ratio of trans to gauche conformers in the alkyl chain. The higher the shifts, the higher the ratio of trans to gauche there. The higher the quantity of M-HEP that entered the SC lipid region, the more movements the alkyl chain did. It was

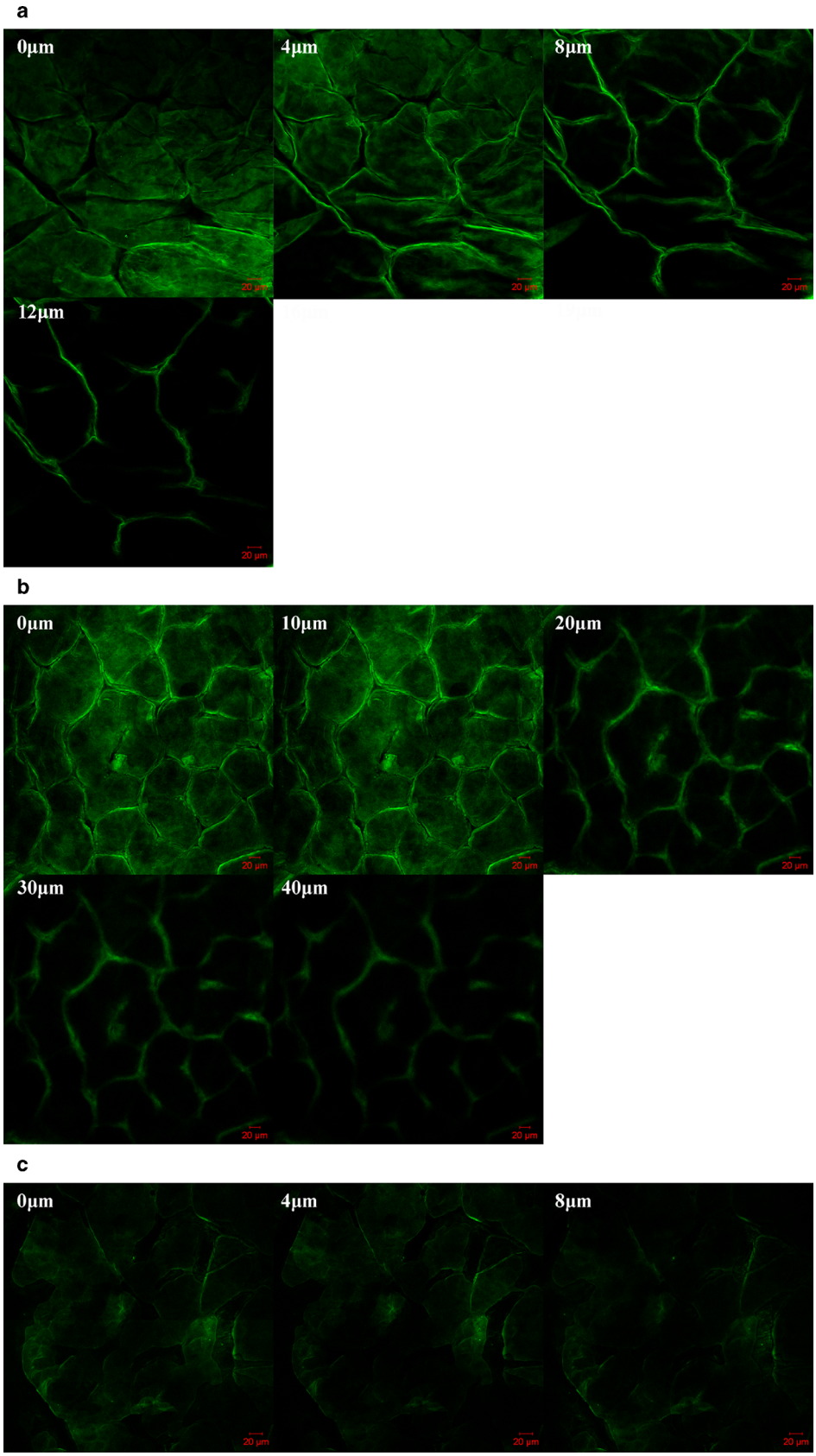

Fig. 3. 2P-LSM images of porcine abdominal skin incubated on a vertical diffusion cell with different vehicles. Fig. 2a 2P-LSM images of porcine abdominal skin incubated on a vertical diffusion cell with 10 % ethanol IPM for 1 h (control). Fig. 2b The images are porcine abdominal skin treated with 20 % M-HEP 10 % ethanol IPM for 1 h. Fig. 2c 2P-LSM images of porcine abdominal skin incubated on a vertical diffusion cell with 20 % M-DEC 10 % ethanol IPM for 1 h. The *scale* is 20 µm

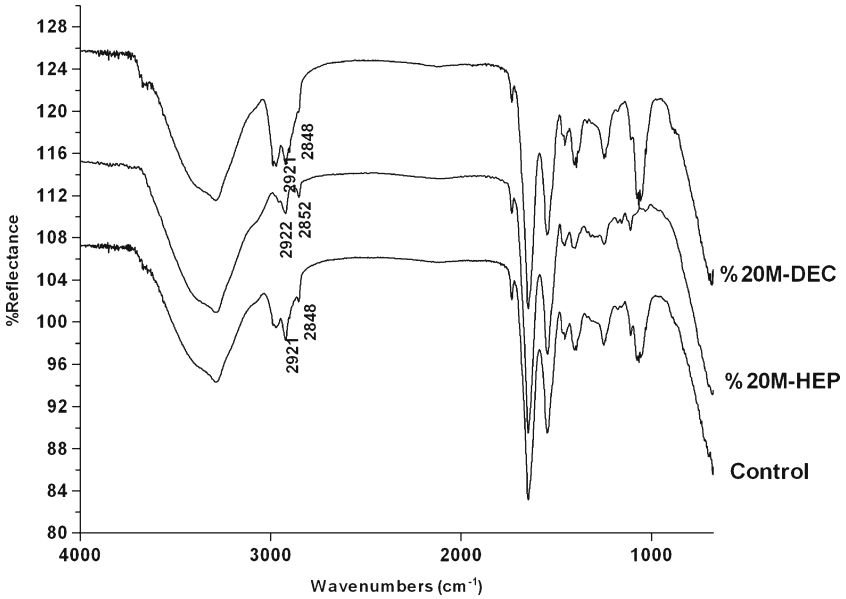

Fig. 4. ATR-FTIR spectra of porcine skin showed asymmetric and symmetric C–H stretching absorbance after enhancer treatment. Enhancer/retardant used was 20 % M-HEP and 20 % M-DEC in combination with 10 % ethanol in IPM, respectively. Untreated by enhancer porcine skin was used as control in this experiment

demonstrated that promoters causing a higher shift of C–H stretching vibration improved drug permeation (8,20). The conformation changes of CER are one of the most important factors to promote TAL penetration. ATR-FTIR spectrum reflected another potential factor existed in the penetration procedure. The amide II near 1,550 cm^{-1} contains mixed N–H in-plane bending and C–N stretching (22). The change of amide II absorption peak after treatment with M-HEP suggested that the amount of α-spiral structure of keratin decreased along with the increase of β-folding structure and nonregulative structure (23). And at the position of 1,000 cm^{-1}, some absorption peaks disappeared, which also indicated the interaction between M-HEP and CER.

Combining with GC results, the retention amounts of M-HEP and M-DEC suggested the interaction between M-HEP and CER. Solubility parameter calculation indicated that M-HEP could easily interact with the polarity region than M-DEC and TAL. The different binding site of enhancers in the lipid region appeared to be another explanation of M-HEP-induced TAL permeation enhancement. Thus, M-HEP provided the highest skin permeation, and it offered the shortest lag time.

The spectrum of M-DEC was the same as that of the control group, implying that M-DEC caused no increase in the movement of the side chain of CER. Solubility parameter calculation indicated that M-DEC was prone to interact with the nonpolarity region than M-HEP. Combined with *in vitro* penetration results, TAL penetration induced by M-DEC was hardly detectable. From the 2P-LSM images, there was little fluorescein penetration 8 μm beneath the skin surface. The results of ATR-FTIR suggested that M-DEC could not enhance the motion of the alkyl chain but occupy the space where TAL could penetrate through the skin. Consequently, when some M-DEC was dissolved in the lipid region, it could not enhance the motion of the alkyl chain but occupy the space where TAL could penetrate through the skin. As a result, TAL penetration was retarded by M-DEC.

CONCLUSION

It is much clearer to elucidate the mechanism of enhancer when the penetrant is regarded as a crucial factor to the permeation procedure. The 2P-LSM images reflected the action sites and enhancement efficiency of M-HEP and M-DEC. Meanwhile, ATR-FTIR spectra demonstrated the frequency changes of CER in the lipid domain to explain the distinct permeation behavior of M-HEP and M-DEC. All the results suggested that M-HEP changed the conformation of CER in the lipid region by affecting the microenvironment and increased the fluidization of the lipid region to promote TAL penetration through the skin. M-DEC, on the other hand, does not modify the CER conformation of the lipid region. The penetrant could affect the penetration procedure of enhancer. The conformation of CER in the lipid region is directly related to the amount of drug permeated.

ACKNOWLEDGMENTS

The program was supported by sub-subject of “new drug creating” of the Mega-Projects for Science Research for the “Eleventh Five-Year Plan” (No. 2009ZX09301-012).

REFERENCES

1. Zhao L, Li Y, Fang L, Ren C, Xu Y, He Z. Effect of *O*-acylmenthol and salt formation on the skin permeation of diclofenac acid. Drug Dev Ind Pharm. 2009;35:814–26.

2. Zhao L, Fang L, Xu Y, Zhao Y, He Z. Effect of *O*-acylmenthol on transdermal delivery of drugs with different lipophilicity. Int J Pharm. 2008;352:92–103.
3. Zhao L, Fang L, Xu Y, Liu S, He Z, Zhao Y. Transdermal delivery of penetrants with differing lipophilicities using *O*-acylmenthol derivatives as penetration enhancers. Eur J Pharm Biopharm. 2008;69:199–213.
4. Yu B, Kim KH, So PT, Blankschtein D, Langer R. Visualization of oleic acid-induced transdermal diffusion pathways using two-photon fluorescence microscopy. J Invest Dermatol. 2003;120:448–55.
5. Yu B, Dong CY, So PT, Blankschtein D, Langer R. In vitro visualization and quantification of oleic acid induced changes in transdermal transport using two-photon fluorescence microscopy. J Invest Dermatol. 2001;117:16–25.
6. Obata Y, Maruyama Y, Takavama K. The mode of promoting activity of *O*-ethylmenthol as a transdermal absorption enhancer. Pharm Res. 2006;23:392–400.
7. Narishetty ST, Panchagnula R. Effect of L-menthol and 1,8-cineole on phase behavior and molecular organization of SC lipids and skin permeation of zidovudine. J Control Release. 2005;102:59–70.
8. Takahashi K, Sakano H, Yoshida M, Numata N, Mizuno N. Characterization of the influence of polyol fatty acid esters on the permeation of diclofenac through rat skin. J Control Release. 2001;73:351–8.
9. Ibrahim SA, Li SK. Chemical enhancer solubility in human stratum corneum lipids and enhancer mechanism of action on stratum corneum lipid domain. Int J Pharm. 2010;383:89–98.
10. Fang L, Kobayashi Y, Numajiri S, Kobayashi D, Sugibayashi K, Morimoto Y. The enhancing effect of a triethanolamine-ethanol-isopropyl myristate mixed system on the skin permeation of acidic drugs. Biol Pharm Bull. 2002;25:1339–44. 17.
11. Hancock BC, York P, Rowe RC. The use of solubility parameters in pharmaceutical solid dosage form design. Int J Pharm. 1997;148:1–21.
12. Seto JE, Polat BE, VanVeller B, Lopez RF, Langer R, Blankschtein D. Fluorescent penetration enhancers for transdermal applications. J Control Release. 2012;158:85–92.
13. Krevelen V, Krevelen DW. Properties of Polymers. Amsterdam: Elsevier; 1990.
14. Dias M, Hadgraft J, Lane ME. Influence of membrane–solvent–solute interactions on solute permeation in skin. Int J Pharm. 2007;340:65–70.
15. Kuo TR, Wu CL, Hsu CT, Lo W, Chiang SJ, Lin SJ, Dong CY, Chen CC. Chemical enhancer induced changes in the mechanisms of transdermal delivery of zinc oxide nanoparticles. Biomaterials. 2009;30:3002–8.
16. Uitto OD, White HS. Electroosmotic pore transport in human skin. Pharm Res. 2003;20:646–52.
17. Alvarez-Román R, Naik A, Kalia YN, Fessi H, Guy RH. Visualization of skin penetration using confocal laser scanning microscopy. Eur J Pharm Biopharm. 2004;58:301–16.
18. Warner KS, Li SK, He N, Suhonen TM, Chantasart D, Bolikal D, Higuchi WI. Structure–activity relationship for chemical skin permeation enhancers: probing the chemical microenvironment of the site of action. J Pharm Sci. 2003;92:1305–22.
19. Warner KS, Li SK, Higuchi WI. Influences of alkyl group chain length and polar head group on chemical skin permeation enhancement. J Pharm Sci. 2001;90:1143–53.
20. Zhang CF, Yang ZL, Luo JB. Effects of cinnamene enhancers on transdermal delivery of ligustrazine hydrochloride. Eur J Pharm Biopharm. 2007;67:413–9.
21. Vaddi HK, Ho PC, Chan SY. Terpenes in propylene glycol as skin-penetration enhancers: permeation and partition of haloperidol, Fourier transform infrared spectroscopy, and differential scanning calorimetry. J Pharm Sci. 2002;91:1639–51.
22. Janůšová B, Zbytovská J, Lorenc P, Vavrysová H, Palát K, Hrabálek A, Vávrová K. Effect of ceramide acyl chain length on skin permeability and thermotropic phase behavior of model stratum corneum lipid membranes. Biochim Biophys Acta. 2011;1811:129–37.
23. He W, Guo X, Zhang M. Transdermal permeation enhancement of *N*-trimethyl chitosan for testosterone. Int J Pharm. 2008;356(1–2):82–7.